Available online at www.sciencedirect.com
ScienceDirect
Journal of Power Sources 160 (2006) 621–626
JOURNAL OF POWER SOURCES
www.elsevier.com/locate/jpowsour

Additive-containing ionic liquid electrolytes for secondary lithium battery

Jinqiang Xu, Jun Yang*, Yanna NuLi, Jiulin Wang, Zongshuang Zhang

Department of Chemical Engineering, Shanghai Jiao Tong University, Shanghai 200240, PR China

Received 9 October 2005; received in revised form 16 January 2006; accepted 17 January 2006
Available online 24 February 2006

Abstract

Room temperature ionic liquid (RTIL) consisting of *N*-methyl-*N*-propylpiperidinium (PP13) cation and bis(trifluoromethanesulfonyl)imide (TFSI) anion was synthesized and its electrochemical stability was investigated in comparison with 1-butyl-3-methylimidazolium tetrafluoroborate ($BMIBF_4$) and 1-butyl-3-methylimidazolium hexafluorophosphate ($BMIPF_6$). The electrochemical window of PP13-TFSI (5.8 V versus Li/Li^+) is wider than that of $BMIBF_4$ (4.7 V) and $BMIPF_6$ (4.5 V). The cathodic limit of the PP13-TFSI is about −0.3 V versus Li/Li^+, against 0.7 V for $BMIPF_6$ and $BMIBF_4$, so it may be used as the electrolyte for second lithium batteries based on lithium anode. In this work, charge efficiency of lithium plating/striping on nickel substrate and the cycle life have been measured using 0.4 M LiTFSI/PP13-TFSI electrolyte both without and with additives such as vinyl acetate (VA), ethylene sulfite (ES), and ethylene carbonate (EC). Remarkable improvement in cycling efficiency and cycle life was found for EC as additive.

Keywords: Room temperature ionic liquids; Additives; Lithium anode; Cycling efficiency

1. Introduction

There has been an increasing need for lithium ion batteries for the wide range of applications from cellular phones to electric vehicles [1,2]. However, the volatility and inflammability of electrolytes containing organic solvent are serious safety drawbacks. In order to avoid this disadvantage of the electrolyte solution, completely new kind of electrolyte systems should be necessary. On the other hand, lots of attempts have been made to utilize metallic lithium as anode material of lithium secondary batteries, because it offers the largest possible specific energy. But so far the secondary battery based on lithium anode does not succeed. The problems related to low lithium cycling efficiency, dendritic morphology of deposited lithium and safety concerns remain to be solved. It is widely believed that these problems result from the reaction of freshly deposited lithium with the electrolyte components [3]. Some electrolyte additives demonstrate good function to improve the morphology and cycling efficiency of plating lithium [4–7]. Recently, room temperature ionic liquids (RTILs) have been extensively studied as new solvents for electrochemical process due to the extremely low vapor pressure and flame resistance. The unique properties make RTILs attractive candidates for the electrolyte bases of a safe lithium battery. These RTILs are composed of a cation like quaternary ammonium [8], alkylpyridinium [9], alkylpyrrolidinium [10], alkylpyrazolium [11], and alkylimidazolium [12–14] combined with a variety of large anions having a delocalized charge (PF_6^-, BF_4^- and $TFSI^-$). Some of them show the electrochemical stability up to lithium reduction potential (<0 V versus Li/Li^+).

Sakaebe and Matsumoto proposed a novel RTIL, *N*-methyl-*N*-propylpiperidinium bis(trifluoromethanesulfonyl)imide (so-called: PP13-TFSI) as electrolyte base, which exhibited excellent properties in $Li/LiCoO_2$ cell [15]. Recently, they reported the charge–discharge properties of $Li/LiCoO_2$ cell using several RTILs with different amide anions and aliphatic onium cations and it was revealed that the structure and classification of the anionic and cationic species greatly affect the physical properties, such as viscosity, conductivity, and electrochemical stability, which, in turn, exert an influence on the charge and discharge behavior of $Li/LiCoO_2$ cell [16,17]. An efficiently rechargeable $Li/LiCoO_2$ cell battery with RTIL of *N*, *N*-diethyl-*N*-methyl-*N*- (2-methoxyethyl) ammonium bis(trifluoromethylsulfonyl) imide (DEMETFSI) containing LiTFSI as electrolyte was also reported by a different group [18]. The present results indicate that the ionic liquid electrolytes have good anti-oxidation

* Corresponding author. Tel.: +86 21 5474 7667; fax: +86 21 5474 1297.
E-mail address: yangj723@sjtu.edu.cn (J. Yang).

0378-7753/$ – see front matter © 2006 Elsevier B.V. All rights reserved.
doi:10.1016/j.jpowsour.2006.01.054

capability and are well compatible with $LiCoO_2$ cathode. However, it should be realized that not only cathode side, but also anode side is important for potential application of a battery system. Therefore, a comprehensive study on the rechargeability of lithium plating and striping in RTIL-based electrolytes is significant.

Following the previous studies on Li/$LiCoO_2$ cell based on PP13-TFSI electrolyte system [15,16], we focus our research interest in the rechargeability of lithium plating and striping in PP13-TFSI-based electrolytes. Several additives to form good SEI films in secondary lithium cells containing conventional organic electrolytes [19,20] are selected to examine lithium cycling efficiencies in 0.4 M LiTFSI/PP13-TFSI electrolyte.

2. Experimental

2.1. Preparation of RTIL electrolyte

Cations and anions used for RTILs in this study are schematically described with abbreviations in Fig. 1. *N*-methyl-*N*-propylpiperidinium bis(trifluoromethanesulfonyl)imide (PP13-TFSI) was prepared by stirring two aqueous solutions of PP13 (*N*-methyl-*N*-propylpiperidinium)-Br and LiTFSI (Aldrich, as received) at room temperature for 12 h. The amount of LiTFSI was slightly in excess versus that of PP13-Br. PP13-Br was obtained by adding propylbromide (Aldrich, as received) to *N*-methylpiperidine (Aldrich, as received) in acetonitrile at 70 °C with stirring for 24 h. The resulting PP13-TFSI was extracted by CH_2Cl_2 and then the extract was washed with water, that is, adding deionized water into the CH_2Cl_2 solution in a separator funnel with vigorous shaking. After complete dissociation of the water and CH_2Cl_2 layer was confirmed, the CH_2Cl_2 was distilled off using evaporator. Finally, the RTIL was dried in vacuum at 105 °C for 24 h. Finally, the 10 wt% of LiTFSI salt was added to the dried RTIL to form battery electrolyte. This amount corresponds to 0.4 M LiTFSI/PP13-TFSI. The most possible impurity in the electrolyte is bromine anion and water. The measurement of Karl Fischer moisturemeter (mettler-toledo DL39, Swiss) indicates that the water content of the electrolyte is about 16 ppm. Bromine anion was not detected by X-ray fluorescence spectroscopy.

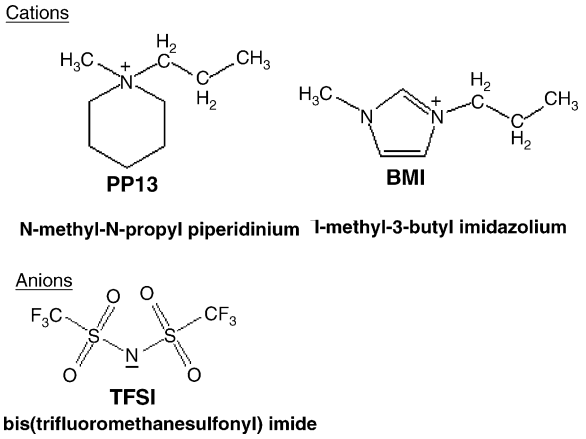

Fig. 1. Schematic illustrations of cationic and anionic species used in this study with their abbreviations.

The other two RTILs, 1-butyl-3-methylimidazolium tetrafluoroborate ($BMIBF_4$) and 1-butyl-3-methylimidazolium hexafluorophosphate ($BMIPF_6$) were commercially available from Aldrich and used after drying in vacuum for 24 h. The chemical structure and some of the physiochemical properties of additives used in this paper are listed in Fig. 2. All of these additives were commercially available from Aldrich and used without further purification.

2.2. Electrochemical measurements

Electrochemical windows of the neat RTILs were measured by linear potential sweep technique. The linear sweep voltammetry (LSV) was performed in three-electrode cells inside an argon-filled glove box (MBRAUN) containing less than 5 ppm each of oxygen and water at room temperature. The working electrode was platinum disk (geometric area = 3.14×10^{-2} cm^2), lithium as both counter and reference electrode.

Redox character of lithium in LiTFSI/PP13-TFSI was examined using cyclic voltammogramms (CVs). It was also conducted in three-electrode cells inside argon-filled glove box at room temperature. The working electrode was nickel piece (surface area 0.1 cm^2), lithium as both counter and reference electrode. The Ni electrode was polished with alumina paste

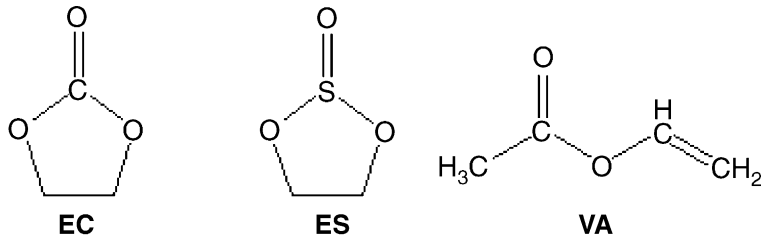

ethylene carbonate	ethylene sulfite	vinyl acetate
m.p. = 36.4°C	b.p. = 68°C	m.p. = -93°C
b.p. = 238°C	Fw = 108.12	b.p. = 72°C
Fw=88.06		Fw=86.09

Fig. 2. Chemical structure and physiochemical properties of additives used in this paper.

($d = 0.1\ \mu m$). Then the polished electrode was washed with deionized water and dried under vacuum.

$Li/LiCoO_2$ coin cell was used to examine the feasibility of ionic liquid electrolyte for rechargeable lithium battery. $LiCoO_2$ electrode was fabricated by spreading the mixture of $LiCoO_2$, acetylene black and PVDF (initially dissolved in *N*-methyl-2-pyrrolidone) with a weight ratio of 85:7:8 onto Al current collector. The cells were charged and discharged between 4.5 and 2.5 V versus the Li counter electrode at a constant current density of $0.05\ mA\ cm^{-2}$.

Lithium cycling efficiencies using Li/Ni coin cell containing LiTFSI/PP13-TFSI with and without additives were checked by a galvanostatic plating–striping technique. The test electrode (area $0.1\ cm^2$) was a Ni piece polished with alumina paste ($d = 0.1\ \mu m$); the counter electrode was a Li sheet. The current density for the cycling was $0.5\ mA\ cm^{-2}$, and the charge of Li plated in each cycle was $1.8\ C\ cm^{-2}$. The cut-off potential for the discharge was 1.0 V versus Li/Li^+. The rest time between stripping and plating was 3 min.

Cycle life of the Li electrode was also evaluated using the above test cell. Lithium was plated on the Ni substrate with a charge of $9\ C\ cm^{-2}$ at the beginning followed by the Li discharge–charge cycles with a constant stripping/plating charge of $0.9\ C\ cm^{-2}$. This procedure means that the depth of discharge (DOD) is 10%. The current density for the initial plating and followed cycling was $0.5\ mA\ cm^{-2}$. The cycle life of the test electrode was evaluated from valid cycle number until the cycle termination, which means that the active Li metal no longer remains on the Ni substrate. As to a practical operation for the termination, each test finished when the discharging voltage reached to 0.3 V versus Li. The mean cycling efficiency (E_m) can be calculated from valid cycle number by using the following equation [3]:

$$E_m = [1 - (Q_p - Q_s)/(Q_s N)] \times 100\%$$

where Q_p is the charge of Li at the initial Li plating ($9\ C\ cm^{-2}$), Q_s is the stripping/plating charge in the subsequent cycles ($0.9\ C\ cm^{-2}$), and N is the valid cycle number.

3. Result and discussion

3.1. Electrochemical windows of ionic liquids

Fig. 3 shows linear sweep voltammograms of three different ionic liquids. The anodic potential of PP13-TFSI is about 5.5 V versus Li/Li^+, a little higher than that of the other two RTILs. A good cathodic stability is seen only for the PP13-TFSI. The cathodic limit potential (E_{cl}) of $BMIPF_6$ and $BMIBF_4$ (both at about 0.7 V versus Li/Li^+) is higher than that of the PP13-TFSI (−0.3 V). Because the decomposition potential of $BMIPF_6$ and $BMIBF_4$ is higher than lithium plating one, these two RTILs could not be used as the electrolytes of the lithium battery using lithium metal or carbon as the anode material. However, the E_{cl} of PP13-TFSI is lower than lithium redox potential and the electrochemical window can reach 5.8 V. It could be expected that PP13-TFSI could work as electrolyte base in the lithium battery system.

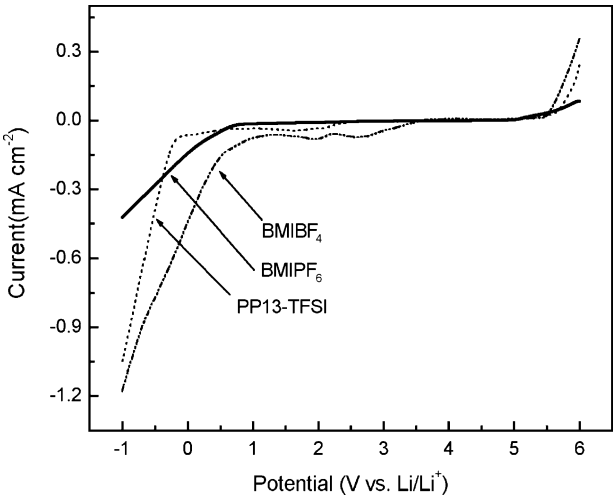

Fig. 3. LSV for three different neat ionic liquids at 20 °C (−1 to 6 V vs. Li/Li^+). Working electrode: Pt, counter electrode and reference electrode: Li. Scan rate: $10\ mV\ s^{-1}$.

3.2. Redox character of lithium in LiTFSI/PP13-TFSI

The cyclic voltammogramm of LiTFSI/PP13-TFSI is shown in Fig. 4. The plating of metallic lithium on Ni substrate can be clearly observed at −0.25 V versus Li/Li^+. The anodic peak at about 0.25 V in the returning scan corresponds to the stripping of lithium. The process presents a typical of overpotential-driven nucleation/growth current loop [21]. This nucleation loop indicates that the electroplating of Li on the Ni electrode during the forward scan requires overpotential in order to initiate the nucleation and subsequent growth of the Li.

Many researchers have studied electrochemical lithium plating and striping on inert metal electrodes in non-aqueous electrolyte solutions and checked the influence of residual water

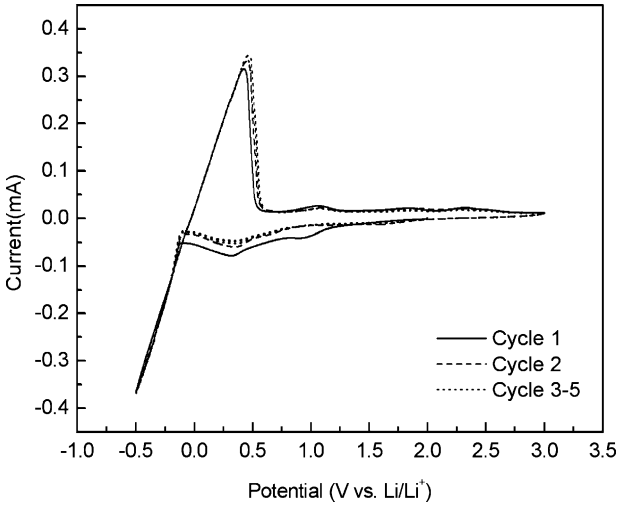

Fig. 4. CVs for ionic liquid electrolyte (LiTFSI/PP13-TFSI) at 20 °C (−0.5 to 3.0 V vs. Li/Li^+). Working electrode: Ni, counter electrode and reference electrode: Li. Scan rate: $10\ mV\ s^{-1}$.

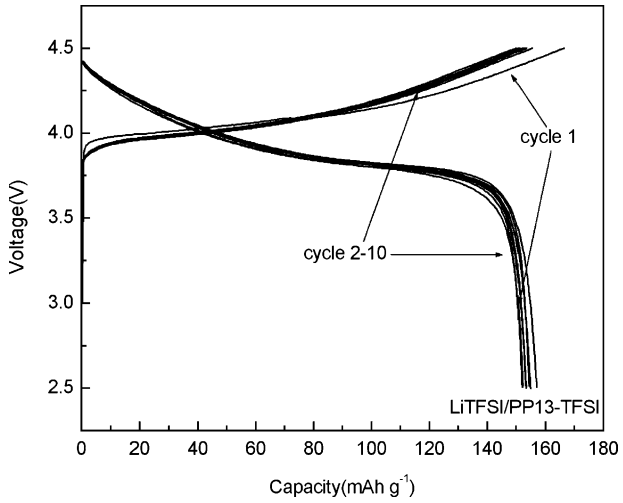

Fig. 5. Charge–discharge curves of Li/$LiCoO_2$ coin cell in 0.4 M LiTFSI/PP13-TFSI at 0.05 mA cm^{-2} with voltage cut-off of 2.5–4.5 V.

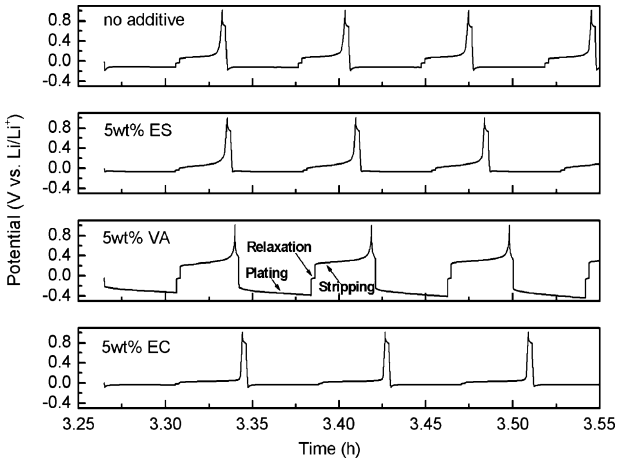

Fig. 6. Typical chronopotentiograms for plating, relaxation and stripping of lithium on nickel substrates in 0.4 M LiTFSI/PP13-TFSI without additive and with 5 wt% VA, ES or EC. The amount of lithium plating was 1.8 C cm^{-2} and current density for plating and stripping was 0.5 mA cm^{-2}.

and O_2 in the electrolytes [22–26]. Most of them reported that dissolved oxygen is reduced at around 2.0 V, and reduction of H_2O occurs in the range 1.0–1.5 V. The couple of the cathodic peak at 0.3 V and the anodic peak at 1.0 V have been generally assigned to underpotential deposition and stripping (UPD and UPS) of lithium on Ni [27,28] and Cu [28], respectively. The voltammograms show two peaks at about 0.9 and 0.3 V except for the lithium plating at −0.25 V in the first cathode sweep. The noticeable peaks above 1.0 V corresponding to reduction of O_2 and H_2O are not observed. The cathodic peak at 0.3 V is attributable to the lithium UPD and the peak at 0.9 V may be assigned to the reductive decomposition of the electrolyte solution. In the second cycle, the peak at 0.9 V disappeared and the cathodic residual current below 1.0 V decreased significantly, suggesting that decomposition of the electrolyte is suppressed but cannot be avoided. The redox character turns to be stable after the initial two cycles.

3.3. Cycle performance of $LiCoO_2$/Li coin cell

Sakaebe et al. have investigated charge and discharge behavior of the cell Li/LiTFSI in PP13-TFSI/$LiCoO_2$ with cut-off of 3.2–4.2 V and affirmed the compatibility of $LiCoO_2$ cathode with LiTFSI/PP13-TFSI electrolyte [15,16]. Here we further enhance voltage upper-limit to 4.5 V to check the rechargeability of $LiCoO_2$ in the electrolyte. As shown in Fig. 5, the charge and discharge characteristics of the cell are equivalent to the half-cell test using the conventional organic electrolyte. The cell has the initial charge capacity of 166 mAh g^{-1} followed by reversible discharge capacity of 152 mAh g^{-1} based on $LiCoO_2$ cathode material, corresponding to charge efficiency of 91.6%. The charge efficiency reaches more than 99.5% after the initial few cycles, while the capacity is stabilized at 150 mAh g^{-1}. An increase of the charge efficiency is associated with improved interfacial property between $LiCoO_2$ cathode and the electrolyte during charge–discharge cycles. The reversible cycling behavior also indicates that the PP13-TFSI electrolyte system has excellent anti-oxidation capability.

3.4. Lithium cycling behaviors

Fig. 6 shows typical voltage profiles for electroplating and stripping of lithium on nickel substrate in 0.4 M LiTFSI/PP13-TFSI and in additive-containing solutions. Lithium plating in the coin cells is controlled by a fixed time period, i.e. fixed charge amount (1.8 C cm^{-2}) at constant current density of 0.5 mA cm^{-2}. Stripping of lithium is controlled by a fixed voltage limit of 1.0 V. For the electrolyte without additive and with 5 wt% EC, an initial overvoltage peak is detected at the beginning of each plating cycle, representing the nucleation overvoltage. Then, it is followed by a region of constant voltage under a constant current density, corresponding to a stable plating progress. On reversal of current, almost constant voltage is kept for the most of the second half-cycle, especially for using EC as the additive. By the end of lithium striping, the voltage rises rapidly, indicating the entire consummation of deposited lithium. When using vinyl acetate (VA) as additive, the voltage polarization for lithium plating/stripping is larger, and the voltage could not maintain constant. This may be contributed to the different composition and structure of the SEI film [20].

Fig. 7 shows the efficiency of lithium cycling versus cycle number in different electrolytes. Common features in all the plots are an enhancement of the efficiency with cycle number in the early stages, possibly due to the removal of reactive impurities from the electrolytes and the formation of surface SEI film [29]. After over 10 cycles, the efficiency for lithium plating and striping turns to be steady. Without additives, the steady cycling efficiency is around 60%. The poor cycling performance appears unmatchable to the wide electrochemical window of PP13-TFSI. Besides difference in the electrochemical conditions, the cell structure, especially the inner pressure, may have some influence on lithium cycling [3]. In our tests, the electrochemical window was measured using three-electrode system without inner pressure, while cycling behavior was checked using coin cells with inner pressure. Moreover, it should be realized that the trace amount of impurity in the electrolyte could affect the lithium

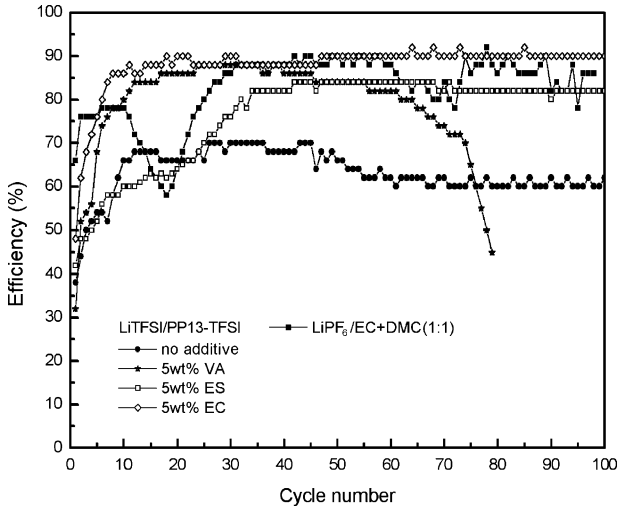

Fig. 7. Cycling efficiencies for plating and striping of lithium on nickel substrates in different electrolytes.

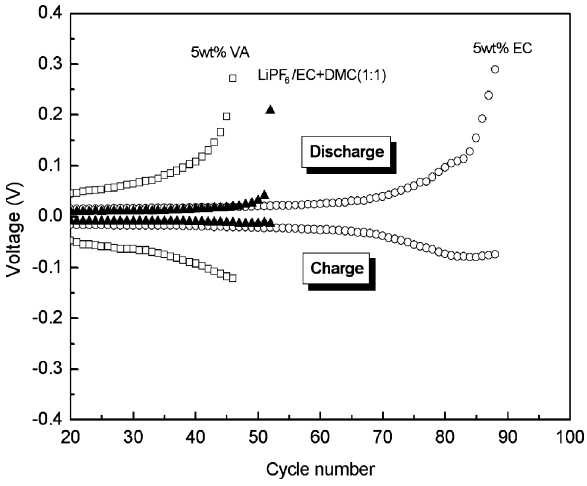

Fig. 8. Voltage changes of Li plating (below 0 V) and stripping (over 0 V) with cycling in 0.4 M LiTFSI/PP13-TFSI electrolyte containing additives and in organic electrolyte (The voltage means maximal one during the half-cycle). Both plating and stripping were carried out at 0.5 mA cm^{-2}.

cycling efficiency. But for the electrochemical window measurement using linear sweep voltammogram, influence of the impurity may be not so sensitive.

As shown in Fig. 7, more or less improvement in cycling efficiency is obtained in the presence of additives. Additive ethylene sulfite (ES) appears to give a slight improvement at initial 30 cycles, then the efficiency can maintain around 80% until the test is terminated at cycle 100. The cycling efficiency using VA as the additive can shortly reach 85% after 10 cycles. But after 60 cycles, the efficiency rapidly drops and the cycling can no longer continue. The best result is related to additive EC with efficiencies around 92% during the steady cycling. On the other hand, a big fluctuation of the efficiency was observed in normal organic electrolyte, which may arise from instable interfacial phenomenon, such as irregular formation and destruction of lithium dendrites, non-uniform surface passivation.

In comparison with the above 100% DOD test, lithium cycling with 10% DOD was further checked in selected electrolytes. The ionic liquid electrolytes without additive and with ES additive are excluded due to the poor result in Fig. 7. The detailed procedure of 10% DOD test is described in Section 2. Fig. 8 exhibits the voltage change during lithium cycling in 0.4 M LiTFSI/PP13-TFSI with 5 wt% VA or EC and in organic electrolyte of 1.0 M $LiPF_6$/EC + DMC (1:1). In the present procedure, an abrupt increase in the discharge voltage until 0.3 V means the termination of the valid cycling. Using the organic electrolyte, 52 cycles are obtained corresponding to a mean efficiency (E_m; see the equation in Section 2) of 82.7%. Using 0.4 M LiTFSI/PP13-TFSI containing 5 wt% EC, 88 cycles are reached with an E_m of 89.8%. The latter presents obvious advantage for lithium cycling. On the other hand, it is noticeable that 10% DOD appears worse than 100% DOD in view of the efficiency and valid cycle number. This may be, at least in part, caused by self-discharge of loaded lithium during the rest time and accumulative surface passivation.

4. Conclusions

PP13-TFSI was synthesized and studied for the use as electrolyte base of rechargeable lithium batteries based on lithium anode, in comparison with commercialized room temperature ionic liquids. The electrochemical measurements indicate that the PP13-TFSI has a wide potential-stable window (>5.5 V). It is well compatible with $LiCoO_2$ cathode and more anti-reductive (the decomposition potential: ca. −0.3 V versus Li/Li^+) than $BMIPF_6$ and $BMIBF_4$. The electrochemical cycling reversibility of lithium plating and striping on Ni substrate is, however, poor using coin cell containing 0.4 M Li-TFSI/PP13-TFSI electrolyte, partly due to reactive impurities and the cell structure. A great improvement can be achieved by adding small amount of ethylene carbonate (EC) into the electrolyte. Lithium cycling with 100% DOD shows a stable efficiency of 90–92% after 10 cycles in the above electrolyte containing 5 wt% EC, against strong fluctuation of the efficiency in 1.0 M $LiPF_6$/EC + DMC (1:1). 10% DOD test also supports the advantage of the ionic liquid electrolyte against the normal organic one for lithium cycling. Nevertheless, for the potential application of the RTILs, more investigation should be done, such as checking morphology change during cycling and further enhancing the charge efficiency, especially during the initial cycles.

Acknowledgements

This work is supported by the National Nature Science Foundation of China (project No. 20373042) and NCET program.

References

[1] N. Terada, T. Yanagi, S. Arai, M. Yoshikawa, K. Ohta, N. Nakajima, A. Yanai, N. Arai, J. Power Sources 100 (2001) 80–92.
[2] T. Iwahori, I. Mitsuishi, S. Shiraga, N. Nakajima, H. Momose, Y. Ozaki, S. Taniguchi, H. Awata, T. Ono, K. Takeuchi, Electrochim. Acta 45 (2000) 1509–1512.

[3] H. Ota, K. Shima, M. Ue, J.-i. Yamaki, Electrochim. Acta 49 (2004) 565–572.
[4] H. Ota, Y. Sakata, Y. Otake, K. Shima, M. Ue, J.I. Yamaki, J. Electrochem. Soc. 151 (2004) A1778–A1788.
[5] R. Mogi, M. Inaba, S.K. Jeong, Y. Iriyama, T. Abe, Z. Ogumi, J. Electrochem. Soc. 149 (2002) A1578–A1583.
[6] M. Ishikawa, S.I. Machino, M. Morita, J. Electroanal. Chem. 473 (1999) 279–284.
[7] K. Saito, Y. Nemoto, S. Tobishima, J. Yamaki, J. Power Sources 68 (1997) 476–479.
[8] H. Mastumoto, H. Kageyama, Y. Miyazaki, Chem. Lett. 2 (2001) 182–183.
[9] Y. Xiao, S.V. Malhotra, J. Organomet. Chem. 690 (2005) 3609–3613.
[10] S. Forsyth, J. Golding, D.R. MacFarlane, M. Forsyth, Electrochim. Acta 46 (2001) 1753–1757.
[11] P.J. Alarco, A.L. Yaser, N. Ravet, M. Armand, Solid State Ionics 172 (2004) 53–56.
[12] K. Ito, N. Nishina, H. Ohno, Electrochim. Acta 45 (2000) 1295–1298.
[13] M. Hirao, K. Ito, H. Ohno, Electrochim. Acta 45 (2000) 1291–1294.
[14] H. Ohno, M. Yoshizawa, W. Ogihara, Electrochim. Acta 48 (2003) 2079–2083.
[15] H. Sakaebe, H. Matsumoto, Electrochem. Commun. 5 (2003) 594–598.
[16] H. Sakaebe, H. Matsumoto, K. Tatsumi, J. Power Sources 146 (2005) 693–697.
[17] H. Matsumoto, H. Sakaebe, K. Tatsumi, J. Power Sources 146 (2005) 45–50.
[18] S. Seki, Y. Kobayashi, H. Miyashiro, Y. Ohno, Y. Mita, A. Usami, N. Terada, M. Watanabe, Electrochem. Solid-State Lett. 8 (2005) A577–A578.
[19] C.X. Wang, H. Nakamura, H. Komatsu, M. Yoshio, H. Yoshitake, J. Power Sources 74 (1998) 142–145.
[20] K. Abe, H. Yoshitake, T. Kitakura, T. Hattori, H.Y. Wang, M. Yoshio, Electrochim. Acta 49 (2004) 4613–4622.
[21] Y.F. Lin, I.W. Sun, Electrochim. Acta 44 (1999) 2771–2777.
[22] M. Moshkovich, Y. Gofer, D. Aurbach, J. Electrochem. Soc. 148 (2001) E155–E167.
[23] D. Aurbach, Y. Cohen, J. Electrochem. Soc. 143 (1996) 3525–3532.
[24] R. Mogi, M. Inaba, T. Abe, Z. Ogumi, J. Power Sources 97–98 (2001) 265–268.
[25] D. Aurbach, Y. Cohen, J. Electrochem. Soc. 144 (1997) 3356–3360.
[26] T. Osaka, T. Momma, Y. Matsumoto, Y. Uchida, J. Power Sources 68 (1997) 497–500.
[27] A. Zaban, D. Aurbach, J. Power Sources 54 (1995) 289–295.
[28] T. Fujieda, Y.Y. Xia, S. Koike, M. Shikano, T. Sakai, J. Power Sources 83 (1999) 186–192.
[29] E. Eweka, J.R. Owen, A. Ritchie, J. Power Sources 65 (1997) 247–251.